Guiding center linear magnetoresistance in the semi-classical regime

Justin C. W. Song[1,2], Gil Refael[1,2], and Patrick A. Lee[3]
[1] Walter Burke Institute for Theoretical Physics and Institute for Quantum Information and Matter, California Institute of Technology, Pasadena, CA 91125 USA
[2] Department of Physics, California Institute of Technology, Pasadena, CA 91125 USA and
[3] Department of Physics, Massachusetts Institute of Technology, Cambridge, MA 02139 USA

We predict that an unconventional guiding center (GC) motion yields a new mechanism for linear and non-saturating (transverse) magnetoresistance in 3D metals. Our theory is semi-classical and applies in the regime where the transport time is much greater than the cyclotron period, and for weak disorder potentials which are slowly varying on a length scale much greater than the cyclotron radius. Under these conditions, orbits with small momenta along magnetic field B are partially trapped and dominate the transverse conductivity. When disorder potentials are stronger than the Debye frequency, linear magnetoresistance is predicted to survive up to room temperature and beyond. We argue that the new GC magnetoresistance mechanism accounts for the recently observed giant linear magnetoresistance seen in 3D Dirac materials.

Magnetoresistance provides a powerful means with which to probe the scattering history of particles in a magnetic field. Departure from the conventional paradigm - quadratic magneto-resistance at low fields, saturating at high fields [1] - signals anomalous particle scattering behavior. One particularly appealing regime is non-saturating and linear magnetoresistance (LMR), which has a long standing history given its potential for disruptive technological impact [2–5].

Very few theories predict LMR in a single component metal. A well known example is Ref. [2], which showed that Dirac metals in the extreme quantum limit (when only the $n = 0$ Landau level is occupied) exhibit LMR in the presence of screened Coulomb impurities. Recently, Klier et al. [6] extended this treatment to finite temperatures and short range impurities, but restrict their attention to chemical potential μ at the Dirac point. A second commonly cited LMR mechanism requires strong inhomogeneity [3].

Recently, large LMR that lie outside the above two paradigms was reported [see (i) and (ii) below] in the newly discovered class of three-dimensional Dirac materials (3DDM) [7–11]. LMR in 3DDM exhibit puzzling features including (i) its occurence when multiple Landau levels are occupied far from the extreme quantum limit, and (ii) arising in weakly disordered, high mobility samples. The ubiquity of LMR, manifesting consistently over a variety of 3DDM experimental systems that include TiBiSSe [7], Cd_3As_2 [8, 9], Na_3Bi[10], and TaAs [11] systems, where μ typically lies 0.1 eV above the Dirac point, exposes an urgency for a new mechanism.

Here we propose a novel semi-classical mechanism for non-saturating, and linear magnetoresistance $\rho_{xx}(B)$ wherein charge transport is dominated by guiding center (GC) motion. Importantly, this mechanism naturally gives LMR under (i) and (ii) above. The main requirement is that the disorder potential is smoothly varying on a scale, ξ, which is large as compared with the cyclotron radius, r_c. The main features of GC magnetoresistance

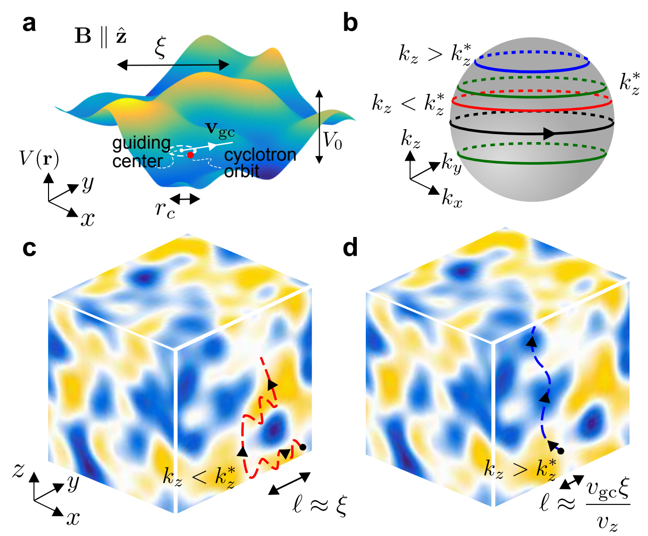

FIG. 1: a) Magnetoresistance can be dominated by guiding center (GC) motion when disorder correlation lengths $\xi \gg r_c$. Here r_c is the cyclotron radius. This regime is characterized by slow GC motion, $\mathbf{v}_{\rm gc} = \nabla_{\mathbf{r}} V(\mathbf{r}) \times \hat{\mathbf{z}}/B$, accompanied by fast cyclotron orbits, $\mathbf{v}_{\rm cycl}$. GC diffusion in this environment givers rise to LMR (see text) b) Electrons perform closed orbits around slices (in k_z) of the Fermi surface. GC motion can be classified into two types, $k_z < k_z^*$ (red), and $k_z > k_z^*$ (blue); k_z^* is indicated by green slice. c) For $k_z < k_z^*$, electrons are squeezed in z yielding mean free paths $\ell \approx \xi$ and in-plane $D_{xx} \sim v_{\rm gc}\xi \propto 1/B$ (see text). d) In contrast, $k_z > k_z^*$ electrons exhibit unconstrained z motion yielding in-plane $D_{xx} \sim v_{\rm gc}^2\xi/v_z \propto 1/B^2$ (see text).

are exposed by writing the transverse resistivity as

$$\rho_{xx} = \frac{\sigma_{xx}}{\sigma_{xx}^2 + \sigma_{xy}^2} = \frac{\mathcal{G}}{\sigma_{xy}}, \quad \mathcal{G} = \frac{\tan\theta_H}{1 + [\tan\theta_H]^2}, \qquad (1)$$

where σ_{xx} and σ_{xy} are the transverse (x-y plane) conductivity and Hall conductivities respectively, and $\tan\theta_H = \sigma_{xy}/\sigma_{xx}$ is the Hall angle. Using the familiar $\sigma_{xy} = ne/B$

with n the density, and e the carrier charge, we have

$$\rho_{xx} = \frac{B\mathcal{G}}{ne}. \quad (2)$$

As we argue below, in the regime of $\omega_c \tau_{\rm tr} \gg 1$ and $\xi \gg r_c$, unconventional GC diffusion gives a Hall angle, and therefore $\mathcal{G}$, that is *independent* of magnetic field, leading to LMR in Eq. (2). Here ω_c is the cyclotron frequency, and $\tau_{\rm tr}$ is the transport time.

Guiding center magnetoresistance can be understood as follows. In semi-classically large B fields ($\omega_c \tau_{\rm tr} \gg 1$), electrons exhibit in-plane trajectories $\mathbf{r}_\perp(t)$ characterized by slow guiding center motion $\mathbf{R}_{\rm gc}(t)$ accompanied by fast cyclotron orbits $\mathbf{r}_{\rm cycl}(t)$. The latter, characterized by r_c, depends on intrinsic material properties and B; whereas the former depends on the potential profile sampled by the electron over one cycle which can yield unusual trajectories [12]. A unique situation arises for slowly varying disorder potentials $V(\mathbf{r})$. In this regime $\xi \gg r_c$ (see Fig. 1a), electron trajectories are dominated by guiding center motion which follows the local disorder landscape at $R_{\rm gc}$, with velocity $\mathbf{v}_{\rm gc} = [\nabla_{\mathbf{R}_{\rm gc}} V(\mathbf{R}_{\rm gc})] \times \hat{\mathbf{z}}/B$.

Guiding center diffusion is characterized by diffusion constant $D_{xx}^{\rm gc} \sim v_{\rm gc}^2 \tau$. The central question is: *what is* τ? First, it is important to note this picture is not valid in strictly 2D, because GCs form closed orbits along equipotential lines. Hence it is crucial to include motion in the z direction which restores diffusive motion. There are two classes of electron motion depending on their k_z value with respect to k_z^* (Fig. 1b, see also below). For $k_z > k_z^*$, electrons possess kinetic energy in the z direction exceeding the typical potential fluctuation (blue slice, Fig. 1b). As a result, the electron moves freely across many potential fluctuations as shown in Fig. 1d. Within time $\tau_> \approx \xi/v_z$, the GC senses a different local electric field and changes direction. As a result, $D_{xx}^{\rm gc}(k_z > k_z^*) \sim v_{\rm gc}^2 \tau_> \propto 1/B^2$. Using $\sigma_{xy} = ne/B$ and Eq. (1), we recover the standard saturated magnetoresistance.

On the other hand, electrons with $k_z < k_z^*$ (red slice Fig. 1b) are typically trapped or squeezed by a local potential barrier. As shown in Fig. 1c, they must travel sideways by a distance ξ to get around the barrier. In this case, $\tau_< \approx \xi/v_{\rm gc}$ and $D_{xx}^{\rm gc} \sim v_{\rm gc}\xi \sim 1/B$; LMR follows immediately from Eq. (1) and (2). Paradoxically for large B, it is the electrons squeezed in the z direction which dominate transport in the x-y plane, leading to LMR. The importance of squeezed electrons was pointed out by Murzin [13] in the context of magneto-transport of a Boltzmann gas in semiconductors. Here, we adapt his argument to the case of a degenerate Fermi sea and present a more quantitative treatment below.

We emphasize that our mechanism for LMR does not have anything to do with the Dirac spectrum per se. Nevertheless, 3D Dirac semi-metals provide an ideal venue that satisfy the conditions required for LMR. First, the high mobility of 3D Dirac materials ($\eta \gtrsim$ few $\times$ $10^4 \mathrm{cm}^2/\mathrm{Vs}$) allows the regime where electrons undergoes many cyclotron orbits before scattering, $\omega_c \tau_{\rm tr} = B\eta \gg 1$, to be achieved at relatively low magnetic fields. Second, the relatively small chemical potential $\mu \sim 100\,\mathrm{meV}$ *but* large Fermi velocity $v_F \sim 1 - 10 \times 10^8\,\mathrm{cm/s}$ [9], give small cyclotron radius $r_c \sim \mu/ev_F B = 10 - 100\,\mathrm{nm}$ at $1\,\mathrm{T}$. Third, large dielectric constants of $\kappa \sim 40$ [14, 15] effectively screen Coulomb impurities to yield relatively weak and slowly varying disorder potentials, with large correlation lengths, $\xi \sim 20 - 60\,\mathrm{nm}$ [15]. As a result, $\xi \gg r_c$ at relatively low $B \gtrsim 1\,\mathrm{T}$, allowing GC to dominate the x-y plane (transverse) magnetoresistance.

We begin by considering the diffusive motion of charged particles in a magnetic field, $\mathbf{B} = B\hat{\mathbf{z}}$, and a slowly varying and weak disorder potential $V(\mathbf{r})$. While formally interested in 3DDM, our analysis below is general; we will only specify 3DDM as needed to compare to recent experiments. Disorder is characterized by $\langle V(\mathbf{r})V(\mathbf{r}')\rangle = V_0^2 \mathcal{F}(|\mathbf{r}-\mathbf{r}'|/\xi)$, where $\langle \mathcal{O} \rangle$ denotes a disorder average, and ξ the correlation length [21]. Lastly, we will be interested in weak disorder strength $eV_0 < \mu$ as evidenced by the high mobility of 3DDM [7–11], and recent estimates [15].

Equations of motion - The motion of particles on the Fermi surface with chemical potential μ can be described by the semi-classical equations of motion for each k_z slice (Fig. 1b)

$$m\dot{\mathbf{v}}_\perp = -e\nabla_{\mathbf{r}} V(\mathbf{r}) + e\mathbf{v}_\perp \times \mathbf{B}, \quad (3a)$$

$$m\dot{v}_z = -e\partial_z V(\mathbf{r}), \quad (3b)$$

where m is the cyclotron mass, $\mathbf{v}_\perp(k_z, \mu) = (v_x, v_y)$, and $v_z(k_z, \mu)$ are velocities transverse to the magnetic field and along the magnetic field respectively. We note that throughout our analysis below, these quantities depend on momentum along the field, k_z, and μ. For e.g., the x-y plane speed for Dirac particles is $|\mathbf{v}_\perp| = v_0 = v_F\sqrt{1 - k_z^2/k_F^2}$, and the cyclotron mass is $m = \mu/v_F^2$ [16], where v_F is the Fermi velocity, and k_F the Fermi wave vector. For brevity in notation, in what follows we will drop explicit mention of k_z dependence, bringing it up when necessary.

The trajectories of charged particles, $\mathbf{r}(t)$, in crossed $\mathbf{B}$ and $V(\mathbf{r})$ can be complex, since they involve transport processes that span multiple time scales (e.g., cyclotron period, $1/\omega_c$, guiding center scattering time τ (see below), and transport time, $\tau_{\rm tr}$). However, in semi-classically strong fields ($\omega_c \tau_{\rm tr} \gg 1$), and for a slowly varying potential so that correlation length is larger than cyclotron radius ($\xi \gg r_c$), its motion is conveniently captured via $\mathbf{r}(t) = \mathbf{R}_{\rm gc}(t) + \mathbf{r}_{\rm cycl}(t)$. Here slow moving $\mathbf{R}_{\rm gc}$ is a three-dimensional vector, whereas fast $\mathbf{r}_{\rm cycl}$ lies in the plane perpendicular to $\mathbf{B}$.

This reasoning yields the following ansatz for velocity in the $\mathbf{r}_\perp = (r_x, r_y)$ plane $\mathbf{v}_\perp$ as [12]

$$\tilde{v}_\perp(t) = v_0 e^{i\omega_c t} + \tilde{v}_{\rm gc}(t), \quad \tilde{v}_{\rm gc} = \frac{i\tilde{E}(\tilde{r}_\perp)}{B}, \tag{4}$$

where $\omega_c = eB/m$, and we have used the complex notation $\mathcal{O}_x + i\mathcal{O}_y = \tilde{\mathcal{O}}$ for motion in the plane perpendicular to $\mathbf{B}$. The latter part of Eq. (4) was obtained by substituting the ansatz into Eq. (3a) and setting $m\dot{v}_{\rm gc} = 0$ since $V(\tilde{r})$ is slowly varying. Eq. (4) is valid for $|m\dot{v}_{\rm gc}| \ll |eE(\tilde{r}_\perp)|$. Estimating $E \approx V_0/\xi$, we obtain the condition

$$\xi^2 \gg \frac{eV_0}{\omega_c^2 m} = r_c^2 \frac{eV_0}{\mu}, \quad \text{where} \quad r_c = \frac{v_0}{\omega_c}. \tag{5}$$

Since we are interested in weak disorder $eV_0 < \mu$ [estimated below, see Eq. (13)], the above condition is satisfied within our regime of validity, $\xi \gg r_c$.

Motion in z can be understood in the following way. First, we note that for $\xi \gg r_c$ and $\omega_c \tau_{\rm tr} \gg 1$, the potential the electron feels is determined by $\langle \mathbf{r}(t)\rangle_{1\,\rm cycle} = \mathbf{R}_{\rm gc}(t)$. Next, for $v_{\rm gc} \ll v_z$ electrons, the GC moves slowly in the x-y plane as compared with z. As a result, integrating Eq. (3b) yields energy conservation

$$\frac{m}{2}\Big\{v_z^2[\mathbf{R}_{\rm gc}(t)] - v_z^2[\mathbf{R}_{\rm gc}(0)]\Big\} = -e\Big\{V[\mathbf{R}_{\rm gc}(t)] - V[\mathbf{R}_{\rm gc}(0)]\Big\}, \tag{6}$$

where we have set $\nabla_{\mathbf{r}_\perp} V(\mathbf{r})\cdot\partial_t \mathbf{r}_\perp = 0$. This is valid when $|\nabla_{\mathbf{r}_\perp} V(\mathbf{r})\cdot\partial_t \mathbf{r}_\perp| \ll |v_z \partial_z V(\mathbf{r})|$. Estimating $|\partial_t \mathbf{r}_\perp| \approx v_{\rm gc}$ and using disorder that is isotropic, yields the original condition $v_{\rm gc} \ll v_z$.

Guiding Center Transport - The separation of time scales between slow GC motion, and fast cyclotron motion enables us to write the velocity correlator as

$$\langle v_\perp(t) v_\perp(0)\rangle \approx \langle v_{\rm gc}(t) v_{\rm gc}(0)\rangle + v_0^2 e^{i\omega_c t - t/\tau_{\rm tr}}, \tag{7}$$

where we have used a simple relaxation-time approximation in the last term to capture the conventional Drude contribution to magnetotransport [12].

In the same way as above, $\mathbf{r}_\perp(t)$ can be replaced with its average over one cycle: $\langle \mathbf{r}_\perp(t)\rangle_{1\,\rm cycle} = \mathbf{R}\perp^{\rm gc}(t)$ since $\xi \gg r_c$, $\omega_c\tau_{\rm tr} \gg 1$. Using Eq. (4), we find GC diffusion, $D_{xx}^{\rm gc} = (1/2)\int_0^\infty \langle v_{\rm gc}(t) v_{\rm gc}(0)\rangle dt$, as

$$D_{xx}^{\rm gc} = \int_0^\infty \langle E[\mathbf{R}_{\rm gc}(t)] E[\mathbf{R}_{\rm gc}(0)]\rangle dt/(2B^2) = E_0^2 \tau/(2B^2),$$
$$\tau = \int_0^\infty dt \mathcal{F}(\Delta R_{\rm gc}/\xi), \tag{8}$$

where $\mathbf{R}_{\rm gc}(t) = [\mathbf{R}_\perp^{\rm gc}(t), R_z^{\rm gc}(t)]$ is the GC trajectory, $\Delta R_{\rm gc} = |\mathbf{R}_{\rm gc}(t) - \mathbf{R}_{\rm gc}(0)|$, E_0 is the characteristic electric field strength of the disorder potential, and τ is the GC motion scattering time which is sensitive to $\mathbf{R}(t)$.

We can adopt a mean-field approach in estimating τ. Since $\mathcal{F}$ rapidly decays for $\Delta R > \xi$, τ is most sensitive to the way the GC moves in $\Delta R(t) < \xi$. As a result, we write $d\Delta R = v_{\rm av} dt$, with the speed $v_{\rm av} = [\langle v_{\rm gc}\rangle_\xi^2 + \langle v_z\rangle_\xi^2]^{1/2}$ averaged over a single domain; here $\langle \mathcal{O}\rangle_\xi$ denotes averaging across a single domain ξ. Changing variables $t \to \Delta R$, we obtain

$$\tau \approx \frac{\xi\mathcal{A}}{\left[\langle v_{\rm gc}\rangle_\xi^2 + \langle v_z\rangle_\xi^2\right]^{1/2}}, \quad \mathcal{A} = \int_0^\infty dx \mathcal{F}(x) \tag{9}$$

where $\mathcal{A}$ is a number of order unity. Using gaussian correlations, $\langle V(x)V(0)\rangle = V_0^2 \mathcal{F}(x) = V_0^2 e^{-x^2/\xi^2}$ we obtain $\mathcal{A} = \sqrt{\pi}/2$, and $E_0^2\xi^2 = 6V_0^2$.

Two distinct classes of GC trajectories can be discerned: (a) where z-motion is squeezed (Fig. 1c), and (b) where z-motion is unrestricted (Fig. 1d). Squeezing in class (a) arises from energy conservation in Eq. (6): for particles with $mv_z^2/2 < V(\mathbf{r})$, the z-direction motion is constrained within a $V(\mathbf{r})$ puddle. It can only escape once x-y plane GC motion diffuses out of a $V(\mathbf{r})$ puddle (see Fig. 1c). Hence, diffusion of these particles along z is squeezed, giving $\langle v_z\rangle_\xi$ that *vanishes* and $v_{\rm av} \approx \langle v_{\rm gc}\rangle_\xi \approx E_0/B$. As a result, Eq. (9) yields $\tau_< \approx \xi\mathcal{A}/\langle v_{\rm gc}\rangle_\xi$ and

$$D_{xx}^{\rm gc} = \frac{E_0\xi\mathcal{A}}{2B}, \quad \text{for} \quad v_z \lesssim (e2V_0/m)^{1/2} = v_*. \tag{10}$$

This corresponds to electrons in Fig. 1b with $k_z < k_z^*$, where k_z^* depends on the dispersion relation and v_*. For e.g., in 3DDM $\hbar k_z^* = (e2V_0\mu/v_F^2)^{1/2}$. We note parenthetically that Eq. (6) can only be used for electrons with $v_z \gg v_{\rm gc}$, see Eq. (6). However, in the opposite limit $v_z \ll v_{\rm gc}$, $\langle v_z\rangle_\xi^2$ is obviously smaller than $\langle v_{\rm gc}\rangle_\xi^2$ in Eq. (9), allowing us to neglect the former's contribution as well, yielding $D_{xx}^{\rm gc}$ as in Eq. (10). As a consistency check, we note that $v_* \gg v_{\rm gc}$ in our regime of validity, $\xi \gg r_c$, $eV_0 < \mu$ [22]. As a result, v_* determines the range of electrons that obey Eq. (10).

In contrast to Eq. (10) above, electrons with $v_z \gtrsim v_*$ do not have z-motion confined [case (b), see Fig. 1d]. As a result, the GC samples many $V(\mathbf{r})$ domains, with its x-y plane velocity scrambled over times $\tau_> \sim \xi/v_z$, yielding an x-y plane mean free path $\ell \sim v_{\rm gc}\xi/v_z$. This is captured in Eq. (9) whence $\langle v_{\rm gc}\rangle_\xi \ll \langle v_z\rangle_\xi$, giving $v_{\rm av} \approx \langle v_z\rangle_\xi \approx v_z$. As a result, Eq. (9) yields $D_{xx}^{\rm gc} \propto 1/B^2$. Importantly, for sufficiently large B, electrons with $v_z > v_z^*$, while very mobile in the z direction, exhibit a suppressed x-y plane mobility as compared with $v_z < v_z^*$ electrons. As a result, (a) dominates the x-y plane transport.

Linear Magnetoresistance in 3DDM - To illustrate the striking effects of GC diffusion we specialize to 3DDM systems. Using the Einstein relation for conductivity $\sigma_{ij} = e^2\nu(\mu)D_{ij}$, and Eq. (10) we obtain

$$\sigma_{xx}^{\rm gc} = e^2 \sum_{k_z} \nu_{\rm 2D}(\mu) D_{xx}^{\rm gc} = \alpha\Big[\frac{1}{B} + \frac{\tilde{B}}{B^2}\Big], \tag{11}$$

where $\alpha/(e^2\nu_{\rm 2D}) = E_0\xi\mathcal{A}k_z^*/(4\pi)$, and $\tilde{B} = (E_0/v_*)\times \ln(k_F/k_z^*)$. Here we have used the 2D density of states for a k_z slice in 3DDM as $\nu_{2D}(\mu) = \mu/2\pi\hbar^2 v_F^2$. We note that the first term dominates over the second when $B > \tilde{B}$. It is useful to re-write this condition as $r_c < \xi\mathcal{K}$, where $\mathcal{K} = \sqrt{2}(\mu/eV_0)^{1/2} \times (\ln[k_F/k_z^*])^{-1} > 1$, since we are interested in $\mu > eV_0$. As a result, we conclude the first term always dominates in our regime of validity, $\xi \gg r_c$.

In the same way, the second term in Eq. (7) yields the usual expressions

$$\sigma_{xx}^{\rm cycl} = \sum_{k_z} \zeta \tau_{\rm tr}, \quad \sigma_{xy} = \sum_{k_z} \zeta \omega_c \tau_{\rm tr}^2 \approx \frac{ne}{B}, \qquad (12)$$

where $\zeta = e^2 \nu_{2D}(\mu) v_0^2/[2(1 + \omega_c^2\tau_{\rm tr}^2)]$; we have taken $\omega_c\tau_{\rm tr} \gg 1$ limit in the last expression. Since $\sigma_{xx}^{\rm cycl} \propto 1/B^2$, for sufficiently large fields it provides a negligible contribution to σ_{xx} as compared with Eq. (11).

An important diagnostic of magentotransport is the Hall angle, $\tan\theta_H = \rho_{xy}/\rho_{xx} = \sigma_{xy}/\sigma_{xx}$. Using Eq. (11) and writing $\sigma_{xx} = \sigma_{xx}^{\rm gc}$ (neglecting $\sigma_{xx}^{\rm cycl}$ contribution since $\omega_c\tau_{\rm tr} \gg 1$), we obtain a B-field independent

$$\tan\theta_H = \frac{2}{\sqrt{27\pi}} \Big(\frac{\mu}{eV_0}\Big)^{3/2}, \qquad (13)$$

where we have used $n = \mu^3/6\pi^2\hbar^3 v_F^3$ for a single fermion flavor in a 3DDM, and used gaussian correlated $\langle V(\mathbf{r})V(\mathbf{r}')\rangle$. Interestingly, the Hall angle can be tuned by V_0 and μ. Estimating $V_0 \approx 20\,\mathrm{mV}$ in 3DDM [15], and using $\mu \sim 0.1\,\mathrm{eV}$ [7–11], we obtain $\tan\theta_H \approx 2.4$.

We note that tunable Hall angle [Eq. (13)] yields a means of controlling $\mathcal{G}$. Indeed, $\mathcal{G}$ is a non-monotonic function of Hall angle (and hence it depends on μ/eV_0), reaching a peak when Hall angle becomes unity.

To summarize, we find that under the conditions $\omega_c\tau_{\rm tr} \gg 1$, $\xi \gg r_c$, $\mu > eV_0$, $\mathcal{G}$ is independent of B field, yielding LMR according to Eq. (2). Of the first two conditions, $\xi \gg r_c$ can be expressed as $B > B_c = mv_F/(e\xi)$ which is a more stringent condition than $\omega_c\tau_{\rm tr} \gg 1$. This is seen by estimating $\tau_{\rm tr}$ using the Born approximation, giving B_c that exceeds the field marking the onset of $\omega_c\tau_{\rm tr} > 1$ by a factor $\sim (\mu/eV_0)^2$. Hence, we predict LMR as long as $B > B_c$.

An important figure of merit for Magnetoresistance is the MR ratio $\mathrm{MR} = \big[\rho_{xx}(B) - \rho_{xx}(0)\big]/\rho_{xx}(0)$. Using Eq. (2), and noting that the mobility $\eta = \sigma_{xx}(0)/ne$, we obtain MR ratio

$$\mathrm{MR} = \frac{\rho_{xx}(B) - \rho_{xx}(0)}{\rho_{xx}(0)} \approx \Big(\frac{\eta[\mathrm{cm}^2/\mathrm{Vs}]}{10^4}\Big) \times B[\mathrm{T}] \times \mathcal{G}. \qquad (14)$$

For typical $\eta \approx 1 - 20 \times 10^4\,\mathrm{cm}^2/\mathrm{Vs}$ in 3DDM samples, Eq. (14) yields giant $\mathrm{MR} \approx 5 - 100$ at $B = 10\,\mathrm{T}$. Here we have used maximal $\mathcal{G} = 1/2$. Importantly, Eq. (14) scales with mobility, mirroring recent observations of LMR in 3DDM [7, 9] where scaling (consistent with Kohler's rule [17]) was observed over a large set of samples, wide range of B fields (up to 60 T [9]), and even at high temperature (up to 300 K in Ref. [8, 9]).

Another intriguing feature of LMR is an unconventional Hall resistivity at large fields. Conventionally, $\rho_{xy}^{(0)} = B/ne$ at large fields and is used to determine the density of carriers. However, since $\sigma_{xx} \propto 1/B$ above, we obtain a Hall resistivity $\rho_{xy} = \sigma_{xy}/(\sigma_{xy}^2 + \sigma_{xx}^2) = \rho_{xy}^{(0)}\mathcal{G}_2$ that differs from the conventional case by a factor $\mathcal{G}_2 = \tan\theta_{\rm H} \times \mathcal{G}$. Since $\mathcal{G}_2 \leq 1$, small Hall angles, can lead to unconventional ρ_{xy}. Indeed, in these situations, determining density through Hall measurements via $n = B/(\rho_{xy}e)$ may overestimate the density.

Inelastic scattering - Energy relaxation through inelastic scattering (e.g. through phonon scattering) in the z-direction can drastically affect GC motion by mixing squeezed z (Fig. 1c) with unconstrained z trajectories (Fig. 1d). Phonon absorption relaxes the energy constraint [Eq. (6)], allowing $v_z < v_*$ electrons to jump out of $V(\mathbf{r})$ troughs. When $\tau_< \approx \xi/v_{\rm gc} \gtrsim \tau_{\rm in}(\varepsilon = V_0 - \frac{m}{2}v_z^2)$, k_z electrons exhibiting squeezed GC motion (Fig. 1c) may escape to unconstrained z motion (Fig. 1d) by absorbing a phonon of energy $\hbar\omega \approx V_0 - \frac{m}{2}v_z^2$. As a result, these electrons exhibit $D_{xx}(k_z) \propto 1/B^2$. Here $\tau_{\rm in}(\varepsilon)$ is the time for an electron to absorb energy ε. While suppressed at low T, Phonon-assisted escape leads to degradation of LMR from 3D GC diffusion when $k_BT \gtrsim V_0$.

However, when typical $V_0 \gg \hbar\omega_{\rm D}$, phonon-assisted escape becomes difficult even at high temperatures since the maximum energy that can be absorbed from phonons is $\hbar\omega_{\rm D} \ll V_0$; ω_D is the Debye frequency. As a result, in this regime LMR is stable even at high temperatures and large fields, as recently observed in Ref. [8, 9] where Cd_3As_2 LMR was observed even at 300 K and high fields.

In the opposite limit, $\hbar\omega_{\rm D}, k_BT > V_0$, inelastic phonon scattering enables facile jumping between equipotential lines. While detrimental to LMR from GC diffusion in 3D, it can have the opposite effect in 2D metals, where GCs conventionally form closed orbits along equipotential lines of a disorder potential yielding localization behavior [18]. For phonon scattering which is not so strong to entirely disrupt the GC motion, but strong enough ($\xi/v_{\rm gc} \gg \tau_{\rm in}$) to induce switching between equipotential, the GC trajectories will become *open*, moving through multiple $V(\mathbf{r})$ domains. We anticipate $D_{xx}^{\rm 2D} \sim v_{\rm gc}\xi \propto 1/B$ and may give LMR in a similar fashion as above. We note LMR has previously been observed in 2D e.g., ultraclean AlGaAs/GaAs heterostructures where large LMR were measured even in the semi-classical regime [19].

Unconventional diffusion of GCs conspires to produce giant LMR. Importantly, the requirements for GC magnetoresistance are modest - arising in the semi-classical regime where multiple Landau levels are occupied, and for weak and smooth disorder. These conditions are readily realized in recently discovered 3DDM in contrast to previous LMR proposals [2, 3, 6, 20]. The giant MR ratios, B-field independent Hall angles that are μ and V_0 tunable, and stability at high temperatures, make

GC diffusion and its magnetoresistance easy to identify in experiment. Indeed, these features bear striking resemblance to LMR measured recently in a variety of 3DDM [7–11]. Additionally, the oscillatory motion of the GC trajectories along B could have interesting, polarization-dependent, absorption signatures in the Terahertz regime. The robustness of GC magnetoresistance mirror the ubiquity of LMR in 3DDM, and will provide a foundation for its future exploitation.

We thank Adam Nahum and Brian Skinner for helpful discussions. JCWS acknowledges support from the Walter Burke Institute for Theoretical Physics as part of a Burke fellowship at Caltech, and the Sherman Fairchild Foundation. GR acknowledges the Packard Foundation and the Institute for Quantum Information and Matter (IQIM). PAL acknowledges the support of the DOE under grant DE-FG01-03-ER46076, and the hospitality of the IQIM while this work was initiated.

[1] J. L. Olsen, *Electron Transport in Metals*, Interscience, New York, (1962).

[2] A. A. Abrikosov, Quantum magnetoresistance, Phys. Rev. B **58**, 2788 (1998).

[3] M. M. Parish and P. B. Littlewood, Non-saturating magnetoresistance in heavily disordered semiconductors, Nature **426**, 162-165 (2003).

[4] Xu, R. et al. Large magnetoresistance in non-magnetic silver chalcogenides. Nature **390**, 57-60 (1997)

[5] M. Lee, T. F. Rosenbaum, M.-L. Saboungi, and H. S. Schnyders, Band-gap tuning and linear magnetoresistance in the silver chalcogenides. Phys. Rev. Lett. **88**, 066602 (2002).

[6] J. Klier, I.V. Gornyi,and A.D. Mirlin, Transversal magnetoresistance in Weyl semimetals, arXiv: 1507.0348 (2015).

[7] M. Novak, S. Sasaki, K. Segawa, and Y. Ando, Large linear magnetoresistance in the Dirac semimetal TlBiSSe, Phys. Rev. B **91**, 041203(R) (2015).

[8] T. Liang, Q. Gibson, M. N. Ali, M. Liu, R. J. Cava and N. P. Ong, Ultrahigh mobility and giant magnetoresistance in the Dirac semimetal Cd_3As_2, Nat. Mat. **14**, 280-284 (2015).

[9] A. Narayanan, M. D. Watson, S. F. Blake, N. Bruyant, L. Drigo, Y. L. Chen, D. Prabhakaran, B. Yan, C. Felser, T. Kong, P. C. Canfield, and A. I. Coldea, Linear Magnetoresistance Caused by Mobility Fluctuations in n-Doped Cd_3As_2, Phys. Rev. Lett. **114**, 117201 (2015).

[10] J. Xiong, S. Kushwaha, J. Krizan, T. Liang, R. J. Cava, and N. P. Ong, Anomalous conductivity tensor in the Dirac semimetal Na_3Bi, arXiv: 1502.06266 (2015).

[11] X. Huang, L. Zhao, Y. Long, P. Wang, D. Chen, Z. Yang, H. Liang, M. Xue, H. Weng, Z. Fang, X. Dai and G. Chen, Observation of the chiral anomaly induced negative magneto-resistance in 3D Weyl semi-metal TaAs, arXiv: 1503.01304 (2015).

[12] C.W.J. Beenaker, Guiding-Center-Drift resonance in a periodically modulated two-dimensional electron gas, Phys. Rev. Lett. **62**, 2020 (1989).

[13] S. S. Murzin, Electron transport in the extreme quantum limit in applied magnetic field, Physics Uspekhi **43**, 349-364 (2000).

[14] J.-P. Jay-Gerin, M.J. Aubin, L.G. Caron, The electron mobility and the static dielectric constant of Cd_3As_2 at 4.2 K, Solid State Communications **21**, 771 (1977).

[15] B. Skinner, Coulomb disorder in three-dimensional Dirac systems, Phys. Rev. B **90**, 060202(R) (2014).

[16] Novoselov, K. S. A., et al. Two-dimensional gas of massless Dirac fermions in graphene, Nature **438**, 197-200 (2005).

[17] A. A. Abrikosov, Fundamentals of the theory of metals, North-Holland (1988).

[18] Editors: R. E. Prange, and S. M. Girvin, *The Quantum Hall Effect*, Springe-Verlag, New York (1987).

[19] V. Renard, Z. D. Kvon, G. M. Gusev, and J. C. Portal, Large positive magnetoresistance in a high-mobility two-dimensional electron gas: Interplay of short- and long-range disorder, Phys. Rev. B **70**, 033303 (2004).

[20] N. Ramakrishnan, M. Milletari, and S. Adam, Magnetoresistance in 3D Weyl Semimetals, arXiv: 1501.03815 (2015).

[21] Slowly varying $V(\mathbf{r})$ can result from coulomb impurities when the screening radius is larger than the inter-impurity distance; for the 3DDM Cd_3As_2 a screening radius of $r_s \sim 40\,\text{nm}$ has been estimated [15], while for typical densities the inter-impurity distances are $n^{1/3} \sim 10\,\text{nm}$.

[22] This can be seen from writing $v_*/v_{\text{gc}} \approx \sqrt{2}(\xi/r_c) \times (\mu/eV_0)^{1/2}$ where we have used Eq. (4) and Eq. (10), and estimated $E_0 \approx V_0/\xi$.